



Cite this: *RSC Adv.*, 2021, **11**, 17715

## Controllable fabrication and self-assembly of Cu nanostructures: the role of Cu<sup>2+</sup> complexes

Lan Yang<sup>a</sup> and Jiangbin Su<sup>ab</sup> 

The controllable fabrication of low dimensional nanostructures and the assembly of nanostructures into hierarchical higher order structures at the atomic or molecular level have been two hot-spots of current nano research. In this work, the fabrication and self-assembly of Cu nanostructures were carried out by reducing Cu<sup>2+</sup> complexes in a mixed aqueous solution of NaOH and hydrazine hydrate at a water bath temperature of 60 °C. The reduction products were characterized using a metalloscope, a scanning electron microscope, a transmission electron microscope and a powder X-ray diffractometer. It was found that the fabrication and self-assembly of Cu nanostructures can be easily realized by controlling the types of Cu<sup>2+</sup> complexes such as [Cu(OH)<sub>4</sub>]<sup>2-</sup>, [Cu(EDA)<sub>2</sub>]<sup>2+</sup> and [Cu(EDA)(OH)<sub>2</sub>]. The authors further analyzed the important roles of Cu<sup>2+</sup> complexes in the fabrication and self-assembly of Cu nanostructures. It was concluded that the Cu<sup>2+</sup> complexes in the aqueous solution would spontaneously arrange into a certain soft template according to the principle of "like dissolves like" and the action of electrostatic forces of positive and negative charges. The as-formed templates determine the fabrication and self-assembly routes and the final products of the Cu nanostructures. Therefore, it provides a controllable and universal method for both fabrication and self-assembly of Cu nanostructures, which may have potential applications in the fields of electronic and optoelectronic nanodevices in the future.

Received 26th March 2021

Accepted 10th May 2021

DOI: 10.1039/d1ra02408f

[rsc.li/rsc-advances](http://rsc.li/rsc-advances)

### 1. Introduction

Nanostructures are usually referred to as structures of materials with sizes below 100 nm, which have some unique physical and chemical properties that distinguish them from conventional bulk materials. Future developments in the frontiers of nanoscale science and technology will greatly depend on the ability to fabricate such low dimensional nanostructures and organize them into hierarchical higher order functional structures.<sup>1</sup> Therefore, the controllable fabrication of low dimensional nanostructures and assembly of nanostructures into hierarchical structures at the atomic or molecular level have been two hot-spots of current nano research. Up till now, many physical and chemical approaches have been employed for the fabrication and assembly of various nanostructures,<sup>2-5</sup> including bimetallic systems and multi-particle systems.<sup>6-10</sup> Among these methods, a solution based synthesis approach<sup>3</sup> is widely regarded as a relatively simple route with the characteristics of low-cost and high-efficiency and is thus welcomed by many researchers. Copper (Cu), as one of the most important metals in modern industry, has attracted considerable attention also in

nanoscale fabrication, especially by the solution phase reduction method.<sup>11-20</sup> In the literature, various Cu nanostructures such as nanoparticles,<sup>11,12</sup> nanowires,<sup>13-15</sup> nanoplates<sup>16,17</sup> and nanotrees<sup>18,19</sup> have been successfully fabricated or assembled by the solution phase reduction approach. Although significant research efforts have been made, there is still a lack of a universal and effective strategy for both fabrication and self-assembly of Cu nanostructures, with precise morphological control. This is because the "bottom-up" growth and self-assembly of nanostructures in chemical solution are extremely non-equilibrium, and are often susceptible to experimental conditions and external environment. In this sense, it is essential to seek a controllable and universal method for both fabrication and assembly of Cu nanostructures. Based on the above consideration, in this work, we particularly studied the fabrication and assembly of Cu nanostructures and tried to seek a controllable and universal approach.

### 2. Experimental details

All the Cu nanostructures were prepared by reducing complexes of Cu<sup>2+</sup> in the mixed aqueous solution of NaOH and hydrazine hydrate (N<sub>2</sub>H<sub>4</sub>·H<sub>2</sub>O) at a water bath temperature of 60 °C. The block diagram in Fig. 1 shows the experimental processes, including preparation and characterization. The preparation procedure can be divided into two steps: (1) the preparation of Cu<sup>2+</sup> complexes; (2) the reduction of Cu<sup>2+</sup> and growth of Cu

<sup>a</sup>College of Science, Jimei University, Xiamen 361021, PR China

<sup>b</sup>Experiment Center of Electronic Science and Technology, School of Microelectronics and Control Engineering, Changzhou University, Changzhou 213164, PR China.  
E-mail: [jbsu@cczu.edu.cn](mailto:jbsu@cczu.edu.cn)

<sup>c</sup>SEU-FEI Nano-Pico Center, Key Laboratory of MEMS of the Ministry of Education, Southeast University, Nanjing 210096, PR China



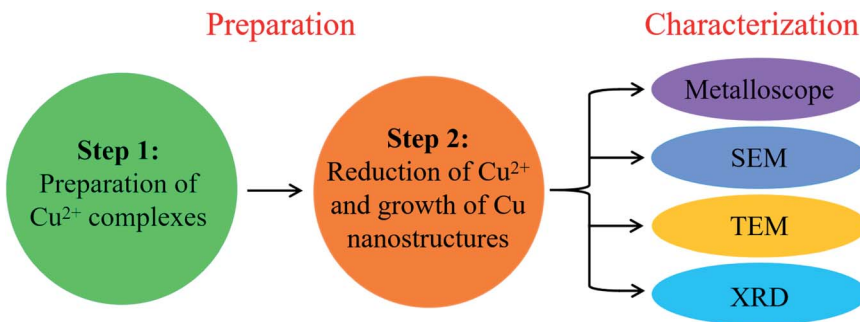


Fig. 1 Block diagram showing the preparation and characterization processes.

Open Access Article. Published on 14 May 2021. Downloaded on 1/20/2026 12:21:40 PM.  
This article is licensed under a Creative Commons Attribution-NonCommercial 3.0 Unported Licence.

CC BY-NC

nanostructures. The reagents included analytical  $\text{Cu}(\text{NO}_3)_2$ , ethylenediamine (EDA), NaOH and  $\text{N}_2\text{H}_4 \cdot \text{H}_2\text{O}$  (85 wt%), whose total volume of aqueous solution was controlled to 30 ml before the reaction. By changing the kinds of  $\text{Cu}^{2+}$  complexes, we have designed six sets of experiments which were labeled as Set 1–6, respectively. (1) Set 1: add 0.03 g  $\text{Cu}(\text{NO}_3)_2$  to  $6.67\text{--}10.5 \text{ mol L}^{-1}$  NaOH solution and heat in water bath for 15 min to form  $[\text{Cu}(\text{OH})_4]^{2-}$  complex, then drop 0.02 ml  $\text{N}_2\text{H}_4 \cdot \text{H}_2\text{O}$  into the mixture to grow for 2 h. (2) Set 2: add 0.03 g  $\text{Cu}(\text{NO}_3)_2$  to deionized water, drop 0.28 ml EDA to this solution and heat in water bath for 15 min to form stable  $[\text{Cu}(\text{EDA})_2]^{2+}$  complex; meanwhile, add 10 g NaOH to deionized water, drop 0.02 ml  $\text{N}_2\text{H}_4 \cdot \text{H}_2\text{O}$  into the NaOH solution and heat in water bath for 15 min; then mix the two solutions and place in the water bath to grow for 2 h. (3) Set 3: add 0.03 g  $\text{Cu}(\text{NO}_3)_2$  to  $6.67\text{--}10.5 \text{ mol L}^{-1}$  NaOH solution to form  $[\text{Cu}(\text{OH})_4]^{2-}$  complex, drop 0.28 ml EDA to this solution and heat in water bath for 15 min to form stable  $[\text{Cu}(\text{EDA})(\text{OH})_2]$  complex, then drop 0.02 ml  $\text{N}_2\text{H}_4 \cdot \text{H}_2\text{O}$  into the mixture to grow for 2 h. (4) Set 4–6: take appropriate amount of the above three complexes, mix them in pairs as 1 : 1, then add the mixed solution of NaOH and  $\text{N}_2\text{H}_4 \cdot \text{H}_2\text{O}$ , and heat them in the water bath for 2 h. In order to facilitate observation, we prepared film samples on glass slides and powder samples on transmission electron microscope (TEM) microgrids, respectively. Subsequently, the metalloscope (MV6000), scanning electron microscope (SEM, JEOL JSM-6360LA) and TEM (JEOL JEM-2100) were used for the surface morphology analysis. In addition, the crystal structure and

chemical composition were also characterized using a powder X-ray diffractometer (XRD, RIGAKU D/Max 2500 PC).

### 3. Results and discussion

Corresponding to the aforementioned different  $\text{Cu}^{2+}$  complexes, as demonstrated in Fig. 2–6, the reduction products were accordingly different. In details, the optical images in Fig. 2(a and b) shows that the reduction products are Cu nanoparticles when the  $\text{Cu}^{2+}$  complex is  $[\text{Cu}(\text{OH})_4]^{2-}$  (Set 1). In the experiment, we further changed the amount of NaOH and found that only particles-like Cu could be obtained. The optical and SEM images in Fig. 3(a–c) demonstrates that the products are Cu nanowires when the  $\text{Cu}^{2+}$  complex is  $[\text{Cu}(\text{EDA})_2]^{2+}$  (Set 2). The XRD pattern in Fig. 3(d) is well consistent with that of synthetic Cu (see JCPDS card no. 04-0836), which confirms the composition of pure Cu in the nanowires. Meanwhile, we can find that the main crystal plane of randomly-oriented Cu nanowire films is (111). It is thus inferred that the growth of Cu nanowires should be along  $\langle 111 \rangle$  direction. The other crystal planes such as (200) and (220) in the XRD pattern can be attributed to the random lateral orientations of Cu nanowires. When the  $\text{Cu}^{2+}$  complexes are  $[\text{Cu}(\text{OH})_4]^{2-}$  and  $[\text{Cu}(\text{EDA})_2]^{2+}$ , the reduction products are Cu nanobranches (remarked as Combination I). In Fig. 4, the optical images in sequence probably show the possible self-assembly process of Combination I: (a) a needle-like nanotwig, (b) a sprouted nanotwig, (c) a two-branched nanotwig and (d) a four-branched nanotwig (or

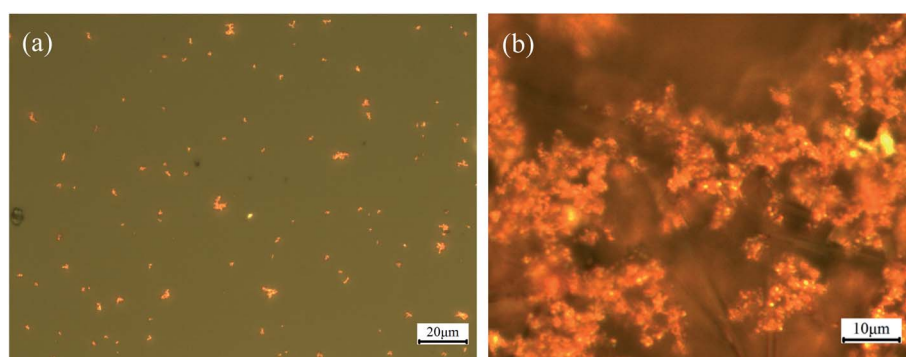


Fig. 2 Optical images showing the morphology of (a) dispersed and (b) aggregated Cu nanoparticles.

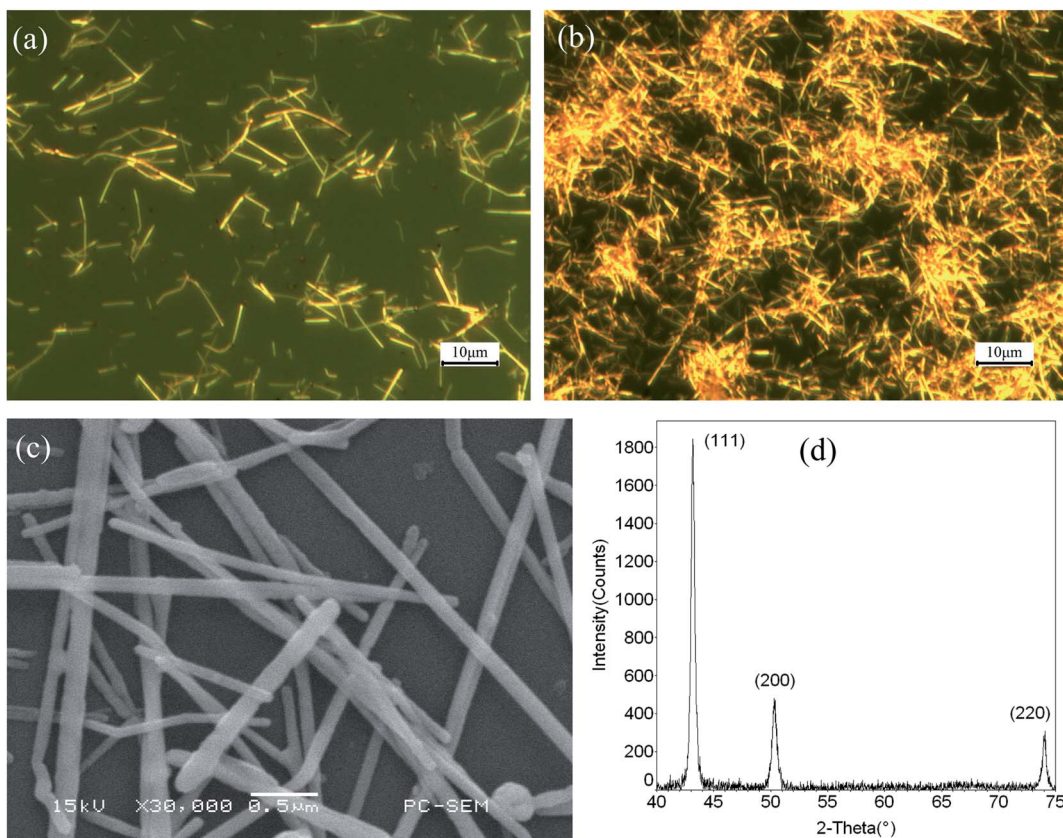


Fig. 3 Optical images showing the morphology of (a) dispersed and (b) aggregated Cu nanowires; SEM image (c) and XRD pattern (d) showing the morphological details and crystal structure of Cu nanowires (film), respectively.

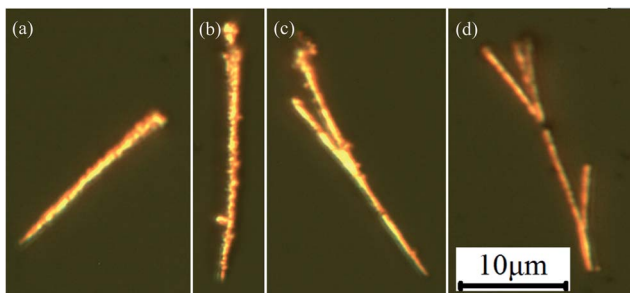


Fig. 4 Optical images in sequence showing the possible self-assembly process of Combination I: (a) a needle-like nanotwig, (b) a sprouted nanotwig, (c) a two-branched nanotwig and (d) a four-branched nanotwig (or nanobranch).

nanobranch). When the  $\text{Cu}^{2+}$  complexes are  $[\text{Cu}(\text{EDA})_2]^{2+}$  and  $[\text{Cu}(\text{EDA})(\text{OH})_2]$ , the reduction products are radially-aligned Cu nanotwigs with a Cu nanoring in the center (remarked as Combination II). The optical image in Fig. 5(a) and TEM image in Fig. 5(b) show the morphology of Combination II and the nodular shape of the building nanotwig and nanoring, respectively. Also note that single Cu nanorings without nanotwigs at the surrounding are also observed in the products (see the arrow in Fig. 5(a)). When the  $\text{Cu}^{2+}$  complexes are  $[\text{Cu}(\text{OH})_4]^{2-}$ ,  $[\text{Cu}(\text{EDA})_2]^{2+}$  and  $[\text{Cu}(\text{EDA})(\text{OH})_2]$ , the reduction products are chrysanthemum-like distribution of Cu nanobranches with

a ring in the center (remarked as Combination III). In Fig. 6, the consecutive optical images show the growth process of combination III: (a) 5 min; (b) 20 min; (c) 45 min; (d) 60 min. It can be found that the self-assembly of Cu nanostructures seems to start from chrysanthemum-like templates, which occupy a territory around them (see Fig. 6(a)). As the reaction proceeds, the Cu ring in the center and the Cu branches around are slowly forming and growing (see Fig. 6(b-d)). Also note that at the beginning, the Cu branches grow preferentially toward the central Cu ring in the form of twigs or wires (see Fig. 6(b and c)). The existence of  $[\text{Cu}(\text{OH})_4]^{2-}$  complexes results in the bifurcation of the Cu twigs, which behaves in a different way from the case without  $[\text{Cu}(\text{OH})_4]^{2-}$  as shown in Fig. 5.

Based on the above findings, we can conclude that the precursors of  $\text{Cu}^{2+}$  complexes play a decisive role in the “bottom-up” growth and self-assembly of Cu nanostructures. By controlling the types of  $\text{Cu}^{2+}$  complexes, various low dimensional nanostructures such as nanoparticles, nanowires, nanorings and their hierarchical higher order structures can be easily achieved. In Fig. 7, the schematic illustrations show the fabrication and self-assembly routes of Cu nanostructures, which are discussed in the following.

(1) When  $\text{Cu}(\text{NO}_3)_2$  is added to excessive NaOH solution,  $[\text{Cu}(\text{OH})_4]^{2-}$  complexes can be formed after sufficient stirring. The  $[\text{Cu}(\text{OH})_4]^{2-}$  complexes are hydrophilic and thus evenly distributed in the aqueous solution. After reduction, the Cu



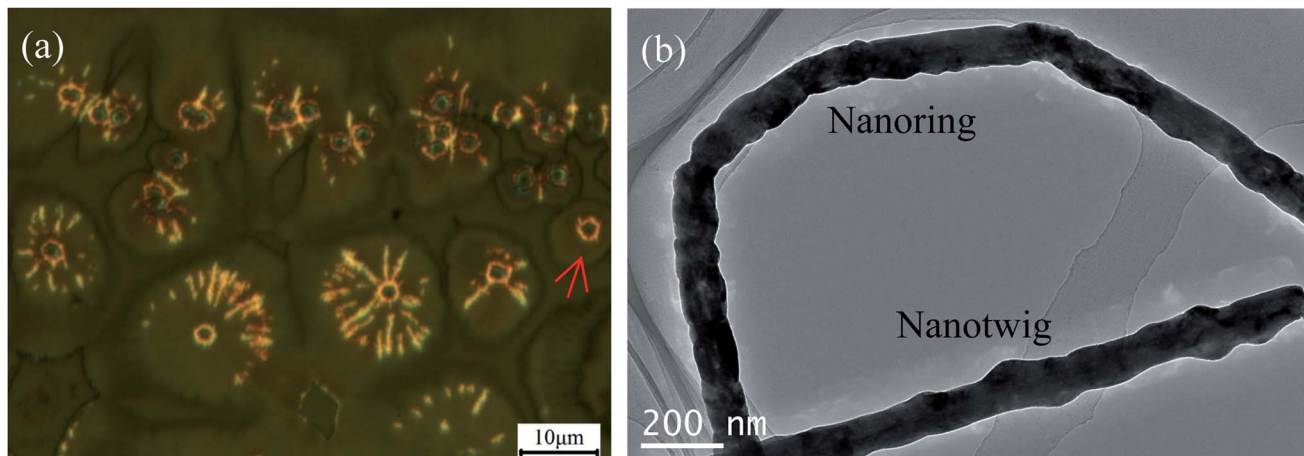


Fig. 5 (a) Optical image showing a single Cu nanoring (see the arrow location) and radially-aligned Cu nanotwigs with a Cu nanoring in the center (remarked as Combination II); (b) TEM image showing the nodular shape of a Cu nanotwig and a Cu nanoring.

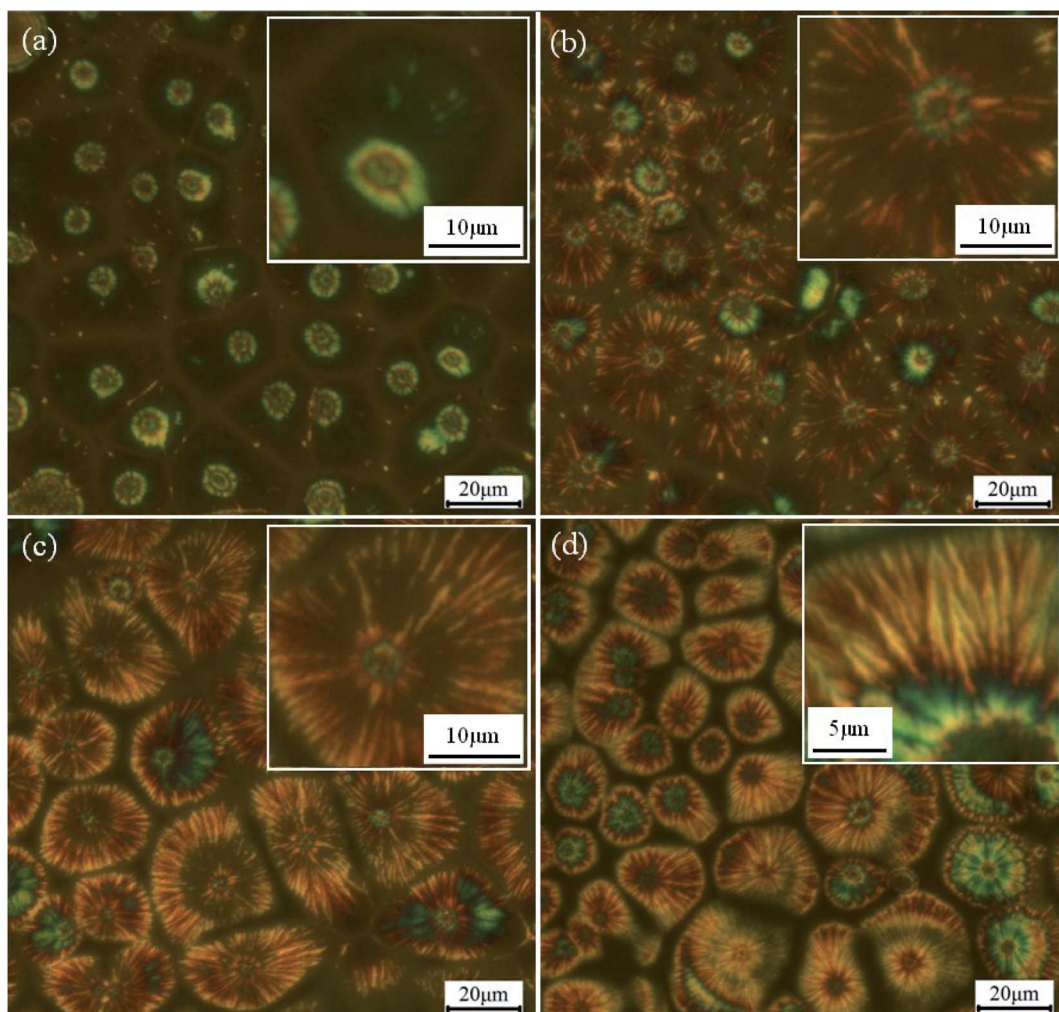


Fig. 6 Consecutive optical images showing the growth process of chrysanthemum-like distribution of Cu nanobranches with a ring in the center (remarked as Combination III): (a) 5 min; (b) 20 min; (c) 45 min; (d) 60 min. The insets are the corresponding images at higher magnifications.

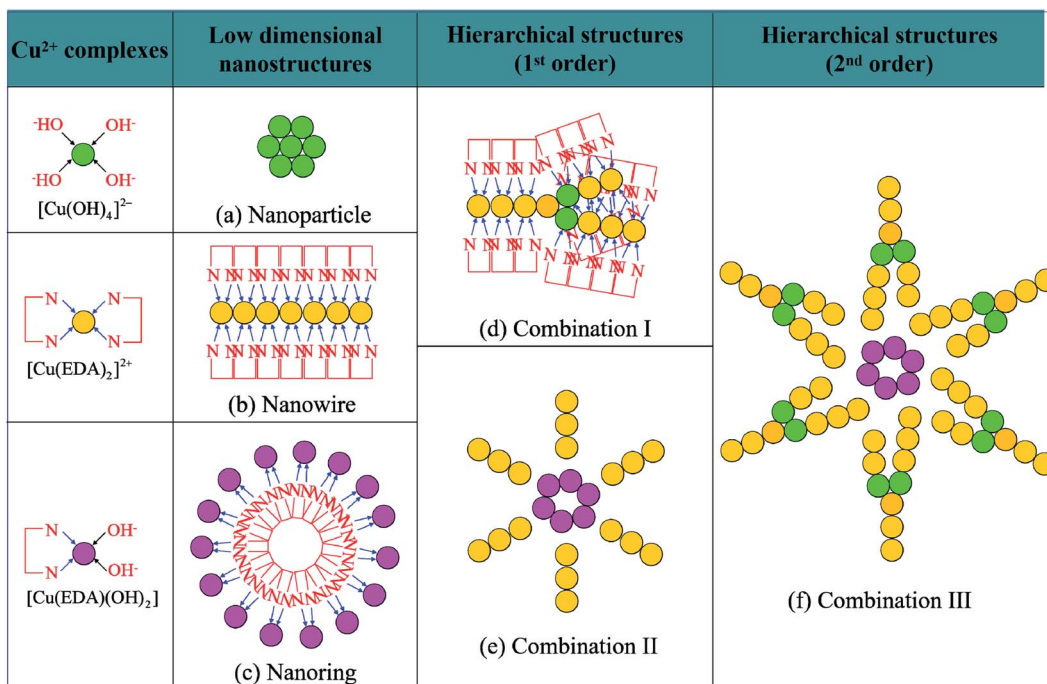


Fig. 7 Schematic illustrations showing the fabrication and self-assembly routes of various Cu nanostructures including: (a) nanoparticles, (b) nanowires or nanotwigs, (c) nanorings, (d) Combination I (nanobranches), (e) Combination II (radially-aligned nanotwigs with a nanoring in the center) and (f) Combination III (radially-aligned nanobranches with a ring in the center).

atoms close to each other will gather together and finally grow into Cu nanoparticles, as shown in Fig. 7(a).

(2) When EDA is added to  $\text{Cu}(\text{NO}_3)_2$  solution,  $[\text{Cu}(\text{EDA})_2]^{2+}$  chelates are formed in the solution.<sup>20,21</sup> Chelate is a complex with ring structure, which is achieved by the chelation of two or more ligands with the same metal ion to form a chelating ring. According to the “like dissolves like” principle,  $[\text{Cu}(\text{EDA})_2]^{2+}$  chelates are arranged into a linear structure, as shown in Fig. 7(b). Due to the steric hindrance effect of the surrounding EDA groups, the Cu atoms can only gather and grow in a straight-line way and one-dimensional Cu nanowires are thus fabricated.

(3) When some EDA is added to  $[\text{Cu}(\text{OH})_4]^{2-}$  solution, the  $[\text{Cu}(\text{OH})_4]^{2-}$  complexes will be replaced by the more stable  $[\text{Cu}(\text{EDA})(\text{OH})_2]$  complexes. Also according to the “like dissolves like” principle, the  $[\text{Cu}(\text{EDA})(\text{OH})_2]$  complexes in the aqueous solution are arranged into circles, as shown in Fig. 7(c). As a result, the reduction products of  $[\text{Cu}(\text{EDA})(\text{OH})_2]$  complexes are Cu nanorings.

(4) If there are some  $[\text{Cu}(\text{OH})_4]^{2-}$  complexes in the  $[\text{Cu}(\text{EDA})_2]^{2+}$  solution, similar to the cases in (a) and (b) of Fig. 7, they will self-assemble into particle-like and linear structures, respectively. During the assembly of  $[\text{Cu}(\text{EDA})_2]^{2+}$  complexes into linear structures, two or more of which may be connected to particle-like  $[\text{Cu}(\text{OH})_4]^{2-}$  complexes due to the electrostatic attraction between positive and negative charges, as shown in Fig. 7(d). As a consequence, the structure of nanobranch Cu (nanobranches, Combination I) is formed. In the products, we can also find some needle-like nanotwigs, which may be caused by the decrease of complex concentration as the reaction proceeds.

(5) When both complexes of  $[\text{Cu}(\text{EDA})_2]^{2+}$  and  $[\text{Cu}(\text{EDA})(\text{OH})_2]$  exist in the solution, the  $[\text{Cu}(\text{EDA})(\text{OH})_2]$  complexes are arranged into circles and the  $[\text{Cu}(\text{EDA})_2]^{2+}$  complexes are arranged radially around the circles, as shown in Fig. 7(e). The formation of such composite structure may be attributed to the electrostatic attraction of  $\text{OH}^-$  around the rings to the  $\text{Cu}^{2+}$  in  $[\text{Cu}(\text{EDA})_2]^{2+}$  complexes. Therefore, the hierarchical structure of radially-aligned Cu nanotwigs with a Cu nanoring in the center (Combination II) are observed in the products.

(6) When complexes of  $[\text{Cu}(\text{OH})_4]^{2-}$ ,  $[\text{Cu}(\text{EDA})_2]^{2+}$  and  $[\text{Cu}(\text{EDA})(\text{OH})_2]$  coexist in the solution, as shown in Fig. 7(f), radially-aligned Cu nanobranches with a Cu ring in the center (Combination III) are finally obtained. In this process, similar to the cases in (c) and (d) of Fig. 7, the combination of  $[\text{Cu}(\text{OH})_4]^{2-}$  and  $[\text{Cu}(\text{EDA})_2]^{2+}$  leads to formation of Cu nanobranches and the  $[\text{Cu}(\text{EDA})(\text{OH})_2]$  leads to formation of Cu nanorings. Meanwhile, the electrostatic attraction between  $\text{OH}^-$  around the rings and the  $\text{Cu}^{2+}$  in  $[\text{Cu}(\text{EDA})_2]^{2+}$  complexes would lead to the combination of Cu nanobranches and Cu nanorings.

In the above processes, the  $\text{Cu}^{2+}$  complexes are arranged into a certain soft template according to the principle of “like dissolves like” and the action of electrostatic force of positive and negative charges. The as-formed templates determine the fabrication and self-assembly routes and the resulting products of Cu nanostructures. Therefore, it provides a controllable and universal method for both fabrication and self-assembly of Cu nanostructures. On the other hand, due to the excellent optical, electrical and mechanical properties,<sup>22,23</sup> the as-prepared Cu nanostructures and their hierarchical higher order structures



may have wide applications in the fields of electronic and optoelectronic nanodevices in the future.

## 4. Conclusions

In this work, the fabrication and self-assembly of Cu nanostructures were realized by reducing  $\text{Cu}^{2+}$  complexes in the mixed aqueous solution of NaOH and hydrazine hydrate. It was found that various Cu nanostructures such as nanoparticles, nanowires and nanorings and their hierarchical higher order structures can be easily achieved by controlling the types of  $\text{Cu}^{2+}$  complexes. It was further concluded that the  $\text{Cu}^{2+}$  complexes in the aqueous solution would spontaneously arrange into a certain soft template according to the principle of "like dissolves like" and the electrostatic force of positive and negative charges. The as-formed templates determine the fabrication and self-assembly routes and the final products of Cu nanostructures. Therefore, it provides a controllable and universal method for the fabrication and self-assembly of Cu nanostructures.

## Conflicts of interest

The authors declare no conflict of interest.

## Acknowledgements

This work was financially supported by Natural Science Foundation of Jiangsu Province (Grant No. BK20191453).

## References

1. A. Murugadoss, R. Pasricha and A. Chattopadhyay, Ascorbic acid as a mediator and template for assembling metallic nanoparticles, *J. Colloid Interface Sci.*, 2007, **311**, 303–310.
2. A. Anders, Metal plasmas for the fabrication of nanostructures, *J. Phys. D: Appl. Phys.*, 2007, **40**, 2272–2284.
3. S. V. N. T. Kuchibhatla, A. S. Karakoti, D. Bera, *et al.*, One dimensional nanostructured materials, *Prog. Mater. Sci.*, 2007, **52**, 699–913.
4. Y. Rahmawan, L. Xu and S. Yang, Self-assembly of nanostructures towards transparent, superhydrophobic surfaces, *J. Mater. Chem. A*, 2013, **1**, 2955–2969.
5. P. D. Halley, R. A. Patton, A. Chowdhury, *et al.*, Low-cost, simple, and scalable self-assembly of DNA origami nanostructures, *Nano Res.*, 2019, **12**, 1207–1215.
6. A. M. Munshi, D. Ho, M. Saunders, *et al.*, Influence of aspect ratio of magnetite coated gold nanorods in hydrogen peroxide sensing, *Sens. Actuators, B*, 2016, **235**, 492–497.
7. D. Hikosou, S. Saita, S. Miyata, *et al.*, Aggregation/self-assembly-induced approach for efficient AuAg bimetallic nanocluster-based photosensitizers, *J. Phys. Chem. C*, 2018, **122**(23), 12494–12501.
8. A. M. Munshi, V. Agarwal, D. Ho, *et al.*, Magnetically directed assembly of nanocrystals for catalytic control of a three-component coupling reaction, *Cryst. Growth Des.*, 2016, **16**(9), 4773–4776.
9. P. Keller and H. Kawasaki, Conductive leaf vein networks produced via Ag nanoparticle self-assembly for potential applications of flexible sensor, *Mater. Lett.*, 2021, **284**, 128937.
10. R. F. Martín, C. Prietzel and J. Koetz, Template-mediated self-assembly of magnetite-gold nanoparticle superstructures at the water-oil interface of AOT reverse microemulsions, *J. Colloid Interface Sci.*, 2021, **581**, 44–55.
11. A. H. Shaik and M. R. Chandan, Preparation of stable copper nanostructures and their direct phase transfer using mercaptosuccinic acid, *Colloids Surf. A*, 2018, **550**, 46–55.
12. C. W. Kim, H. Jeong, Y. Noh, *et al.*, Influence of the chemical molar ratio on the copper nanoparticles: Controlled-surfactants, -reducing agents, and -precursors, *Bull. Korean Chem. Soc.*, 2016, **37**, 700–704.
13. S. Xu, X. Sun, H. Ye, *et al.*, Selective synthesis of copper nanoplates and nanowires via a surfactant-assisted hydrothermal process, *Mater. Chem. Phys.*, 2010, **120**, 1–5.
14. J. F. Chao, Y. Q. Meng, J. B. Liu, *et al.*, Review on the synthesis and antioxidation of Cu nanowires for transparent conductive electrodes, *Nano*, 2019, **14**, 1930005.
15. Y. Wu, M. Gao, S. Li, *et al.*, Copper wires with seamless 1D nanostructures: Preparation and electrochemical sensing performance, *Mater. Lett.*, 2018, **211**, 247–249.
16. S. Xu, S. Xun, Y. Hong, *et al.*, Selective synthesis of copper nanoplates and nanowires via a surfactant-assisted hydrothermal process, *Mater. Chem. Phys.*, 2010, **120**, 1–5.
17. N. D. Kochnev, O. A. Logutenko and A. I. Titkov, Synthesis of nanosized copper plates by reduction of copper with hydrazine hydrate in the presence of an ethoxylated carboxylic acid, *Mater. Today: Proc.*, 2020, **31**, 548–550.
18. C. Hu, Z. Gao and X. Yang, A facile hydrothermal route to synthesis of nonporous and porous hierarchical copper dendrites, *J. Cryst. Growth*, 2007, **306**, 390–394.
19. X. Zhang, G. Wang, X. Liu, *et al.*, Copper dendrites: synthesis, mechanism discussion, and application in determination of L-tyrosine, *Cryst. Growth Des.*, 2008, **8**, 1430–1434.
20. Y. Chang, M. L. Lye and H. C. Zeng, Large-scale synthesis of high-quality ultralong copper nanowires, *Langmuir*, 2005, **21**, 3746–3748.
21. A. R. Rathmell, S. M. Bergin, Y. L. Hua, *et al.*, The growth mechanism of copper nanowires and their properties in flexible, transparent conducting films, *Adv. Mater.*, 2010, **22**, 3558–3563.
22. S. Bhanushali, P. Ghosh, A. Ganesh, *et al.*, 1D copper nanostructures: Progress, challenges and opportunities, *Small*, 2015, **11**, 1232–1252.
23. A. Tamilvanan, K. Balamurugan, K. Ponappa, *et al.*, Copper nanoparticles: Synthetic strategies, properties and multifunctional application, *Int. J. Nanosci.*, 2014, **13**, 1430001.

